Supplementary Information

Brute force determination of the optimum pore sizes for CO_2 uptake†

L. Scott Blankenship,[a*] Nawaf Albeladi,[ab‡] Thria Alkhaldi,[ac‡] Asma Madkhali,[ad‡] and Robert Mokaya[a]

[a] *School of Chemistry, University of Nottingham, University Park, Nottingham, NG7 2RD, UK. Email: leo.blankenship@nottingham.ac.uk*

[b] *Chemistry Department, Faculty of Sciences Yanbu, Taibah University, Yanbu Al Bahr, 46423, Saudi Arabia*

[c] *Department of Chemistry, Jeddah University, Jeddah 23442, Saudi Arabia*

[d] *Department of Chemistry, University College in Samtah, Jazan University, Samtah 86736, Saudi Arabia*

† Electronic Supplementary Information (ESI) available: [Supplementary figures and tables; raw (.aif) isotherms; PSD and modelling analysis summaries as .csv; and raw outputs of D_v, D_π, and D_c for each dataset (.csv)]. See DOI: 00.0000/00000000.

‡ These authors contributed equally to this work.

S1 DataSet 1

Sample code: *PP(xxx)-yTTT*

Where *PP* denotes precursor(s); see table below. *xxx* is used in the case of mixed precursors and denotes the ratio (in %) of second precursor to first. *y* is weight ratio of KOH:precursor. *TTT* is the activation temperature in °C.

Table S1.1 Synthetic information and PSD fitting parameter, λ for samples in dataset 1

Prefix	Number of samples	Precursor	Notes	λ
aP	7	Air carbonised (400 °C) prickly pear		2.5
PUxxx	11	Potassium Hydrogen Phthalate (P), Urea (U)	1 h carbonisation at T	4.0
aT	9	Air carbonised (350 °C) hookah tobacco		3.5
hC	3	Hydrothermally carbonised (350 °C) used cigarette butts	Hydrochar not washed	4.0
hD	3	Hydrothermally carbonised (250 °C) used cigarette butts	Hydrochar washed	4.0

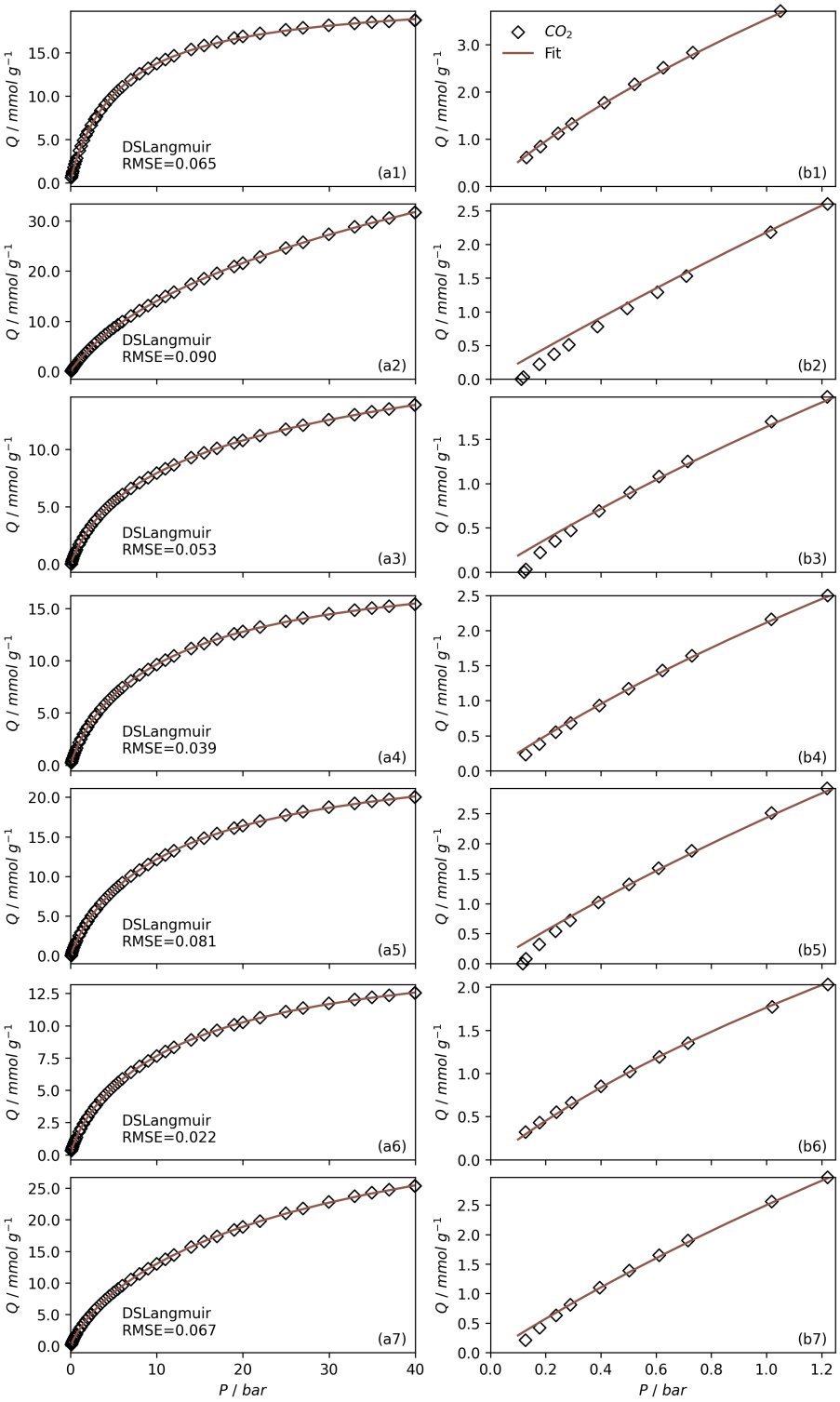

Figure S1.1 CO_2 uptake isotherms and fits in the range 0-40 and 0-1 bar, column (a) and (b) respectively for samples aP-2700, aP-2800, aP-2900, aP-3700, aP-3800, aP-4700, aP-4800 in order in rows (1-7).

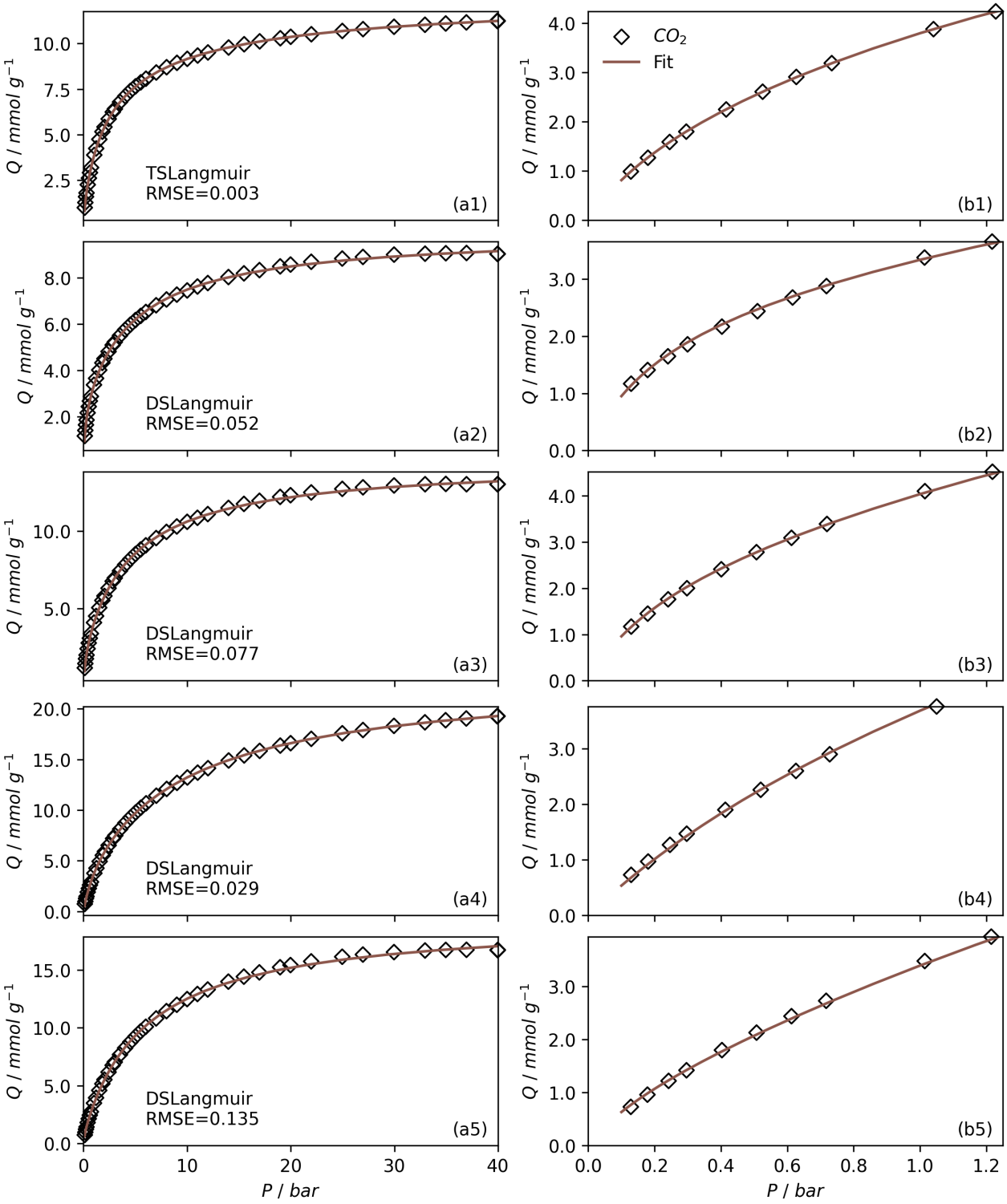

Figure S1.2 CO_2 uptake isotherms and fits in the range 0-40 and 0-1 bar, column (a) and (b) respectively for samples PU000-800, PU025-800, PU025-700, PU025-800, PU025-900 in order in rows (1-5).

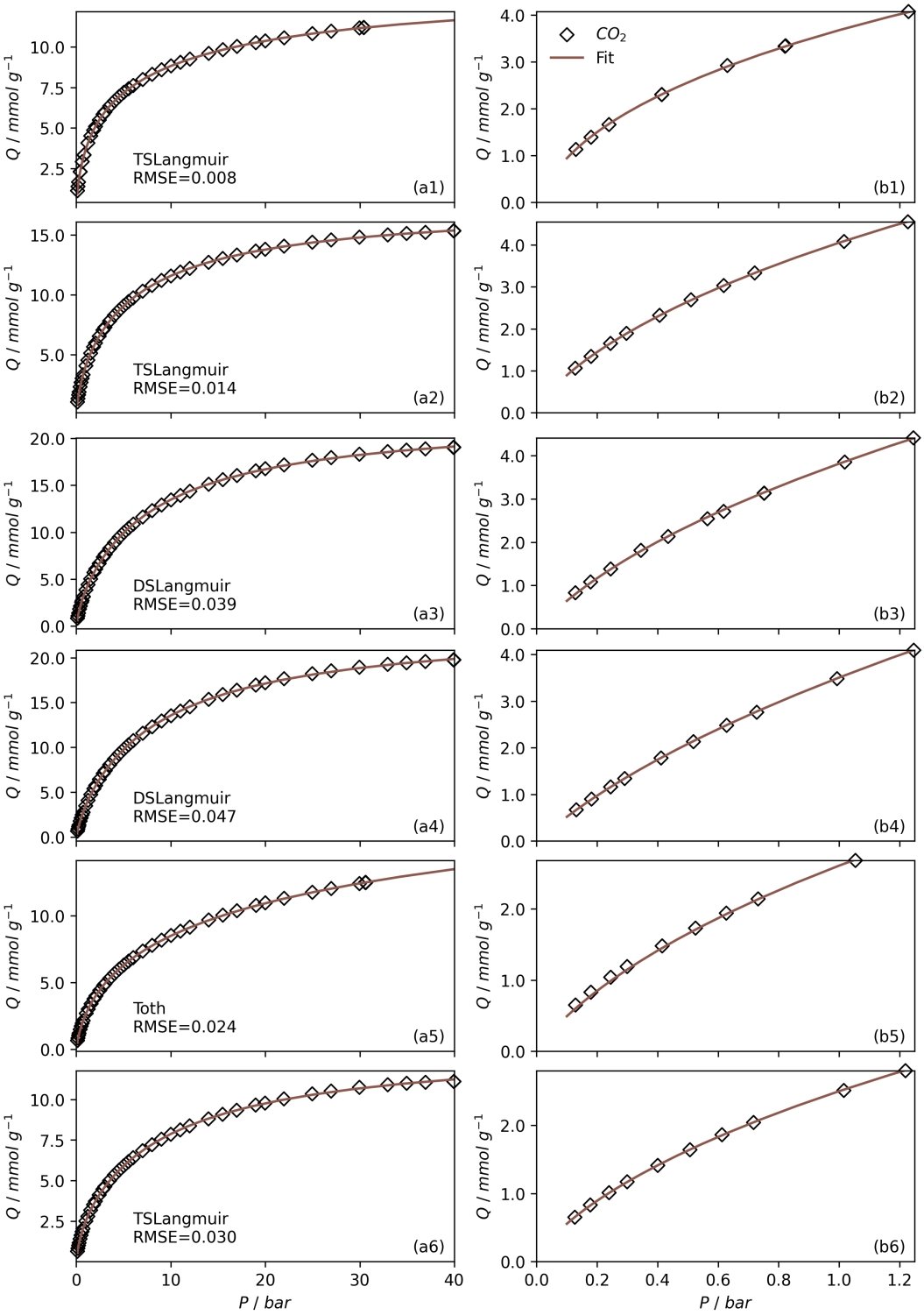

Figure S1.3 CO_2 uptake isotherms and fits in the range 0-40 and 0-1 bar, column (a) and (b) respectively for samples PU050-600, PU050-700, PU050-800, PU050-900, PU100-800, PU100-900 in order in rows (1-6).

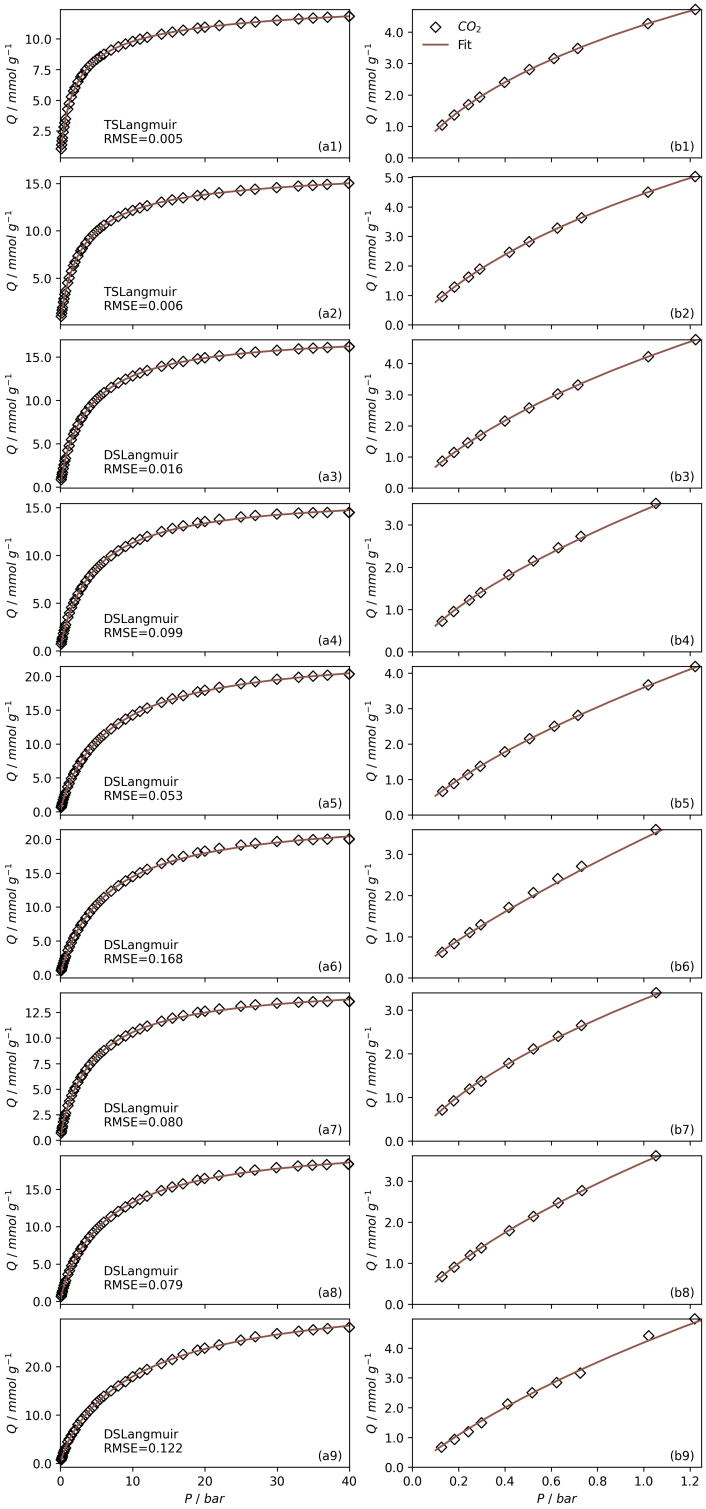

Figure S1.4 CO_2 uptake isotherms and fits in the range 0-40 and 0-1 bar, column (a) and (b) respectively for samples aT-2600, aT-2700, aT-2800, aT-2900, aT-4600, aT-4700, aT-4800, aT-6600, aT-6700, aT-6800 in order in rows (1-9).

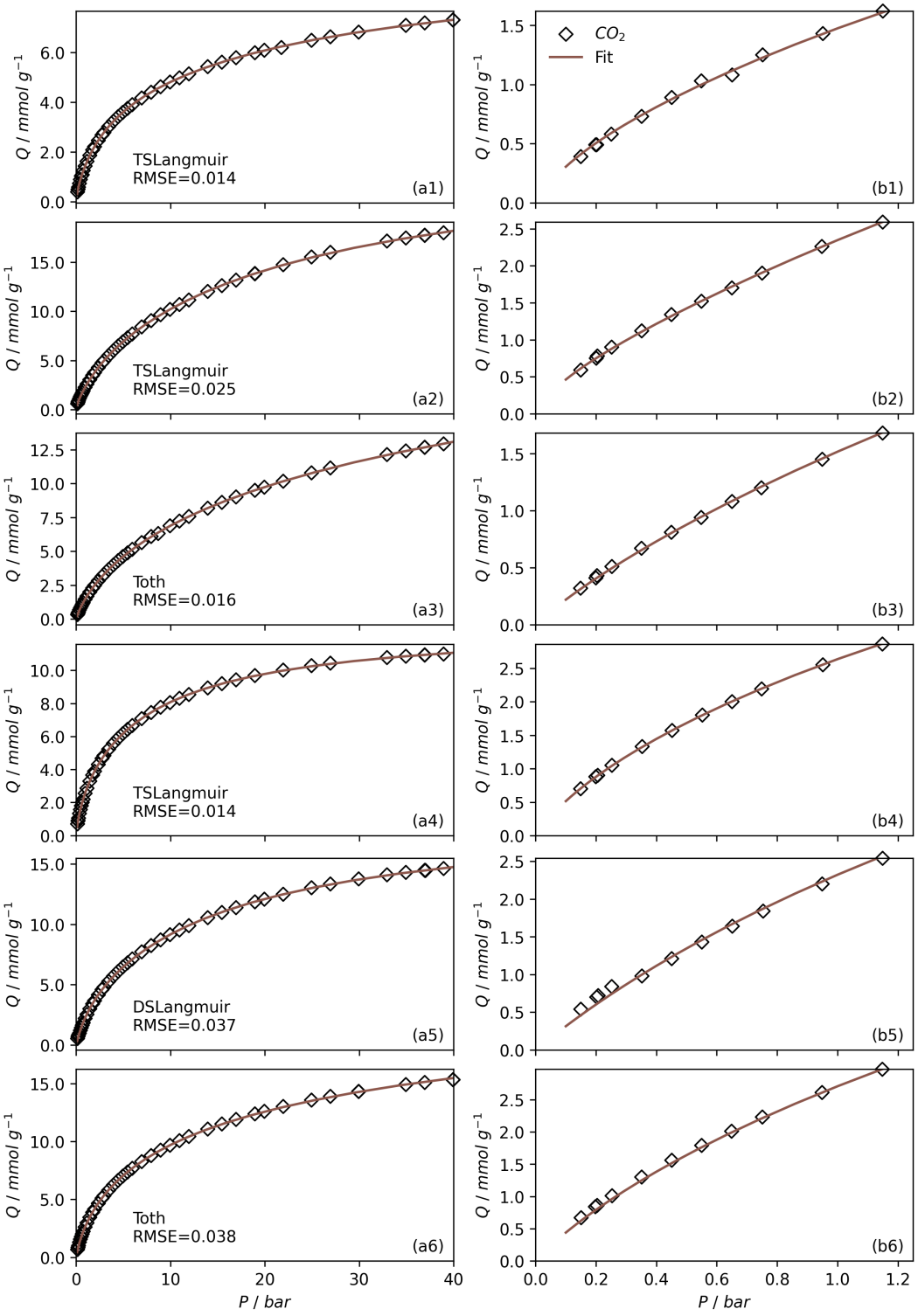

Figure S1.5 CO_2 uptake isotherms and fits in the range 0-40 and 0-1 bar, column (a) and (b) respectively for samples hD-4600, hD-4700, hD-4800, hC-4600, hC-4700, hC-4800 in order in rows (1-6).

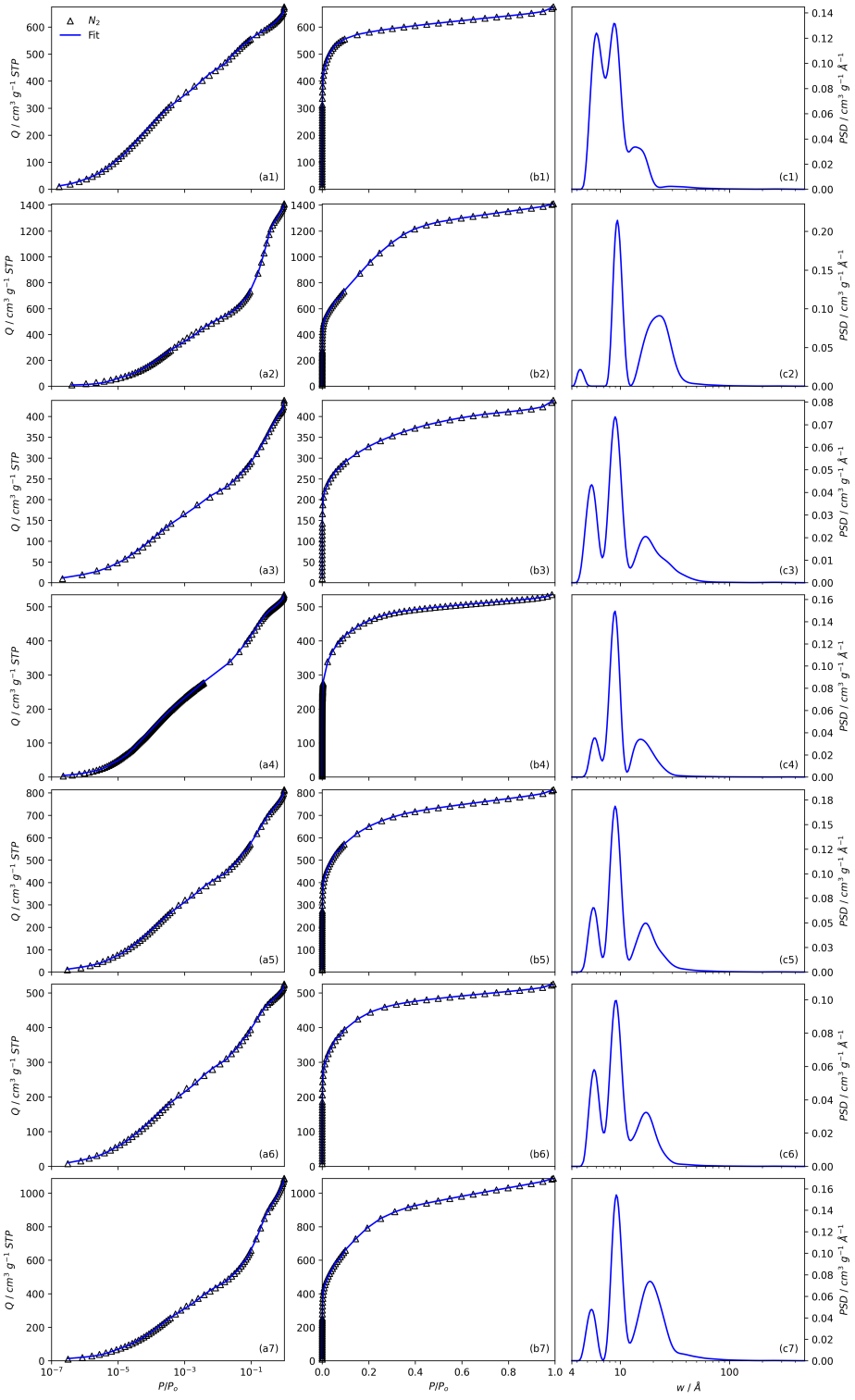

Figure S1.6 Fits to N_2 isotherms with logarithmic (column a) and linear (column b) relative pressure scale, and resultant differential PSDs (column c) for samples aP-2700, aP-2800, aP-2900, aP-3700, aP-3800, aP-4700, aP-4800 in order in rows (1-7).

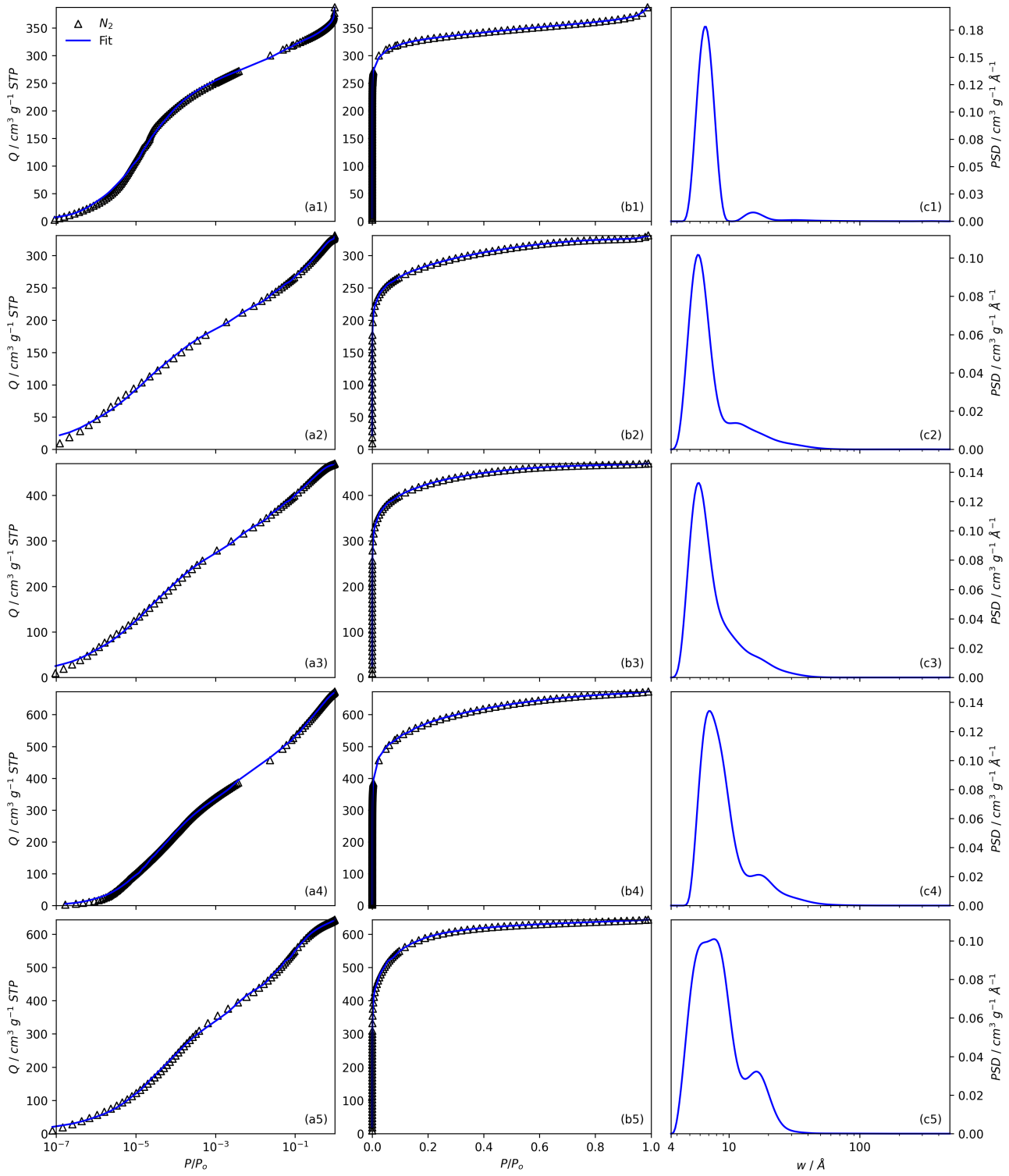

Figure S1.7 Fits to N_2 isotherms with logarithmic (column a) and linear (column b) relative pressure scale, and resultant differential PSDs (column c) for samples PU000-800, PU025-800, PU025-700, PU025-800, PU025-900 in order in rows (1-5).

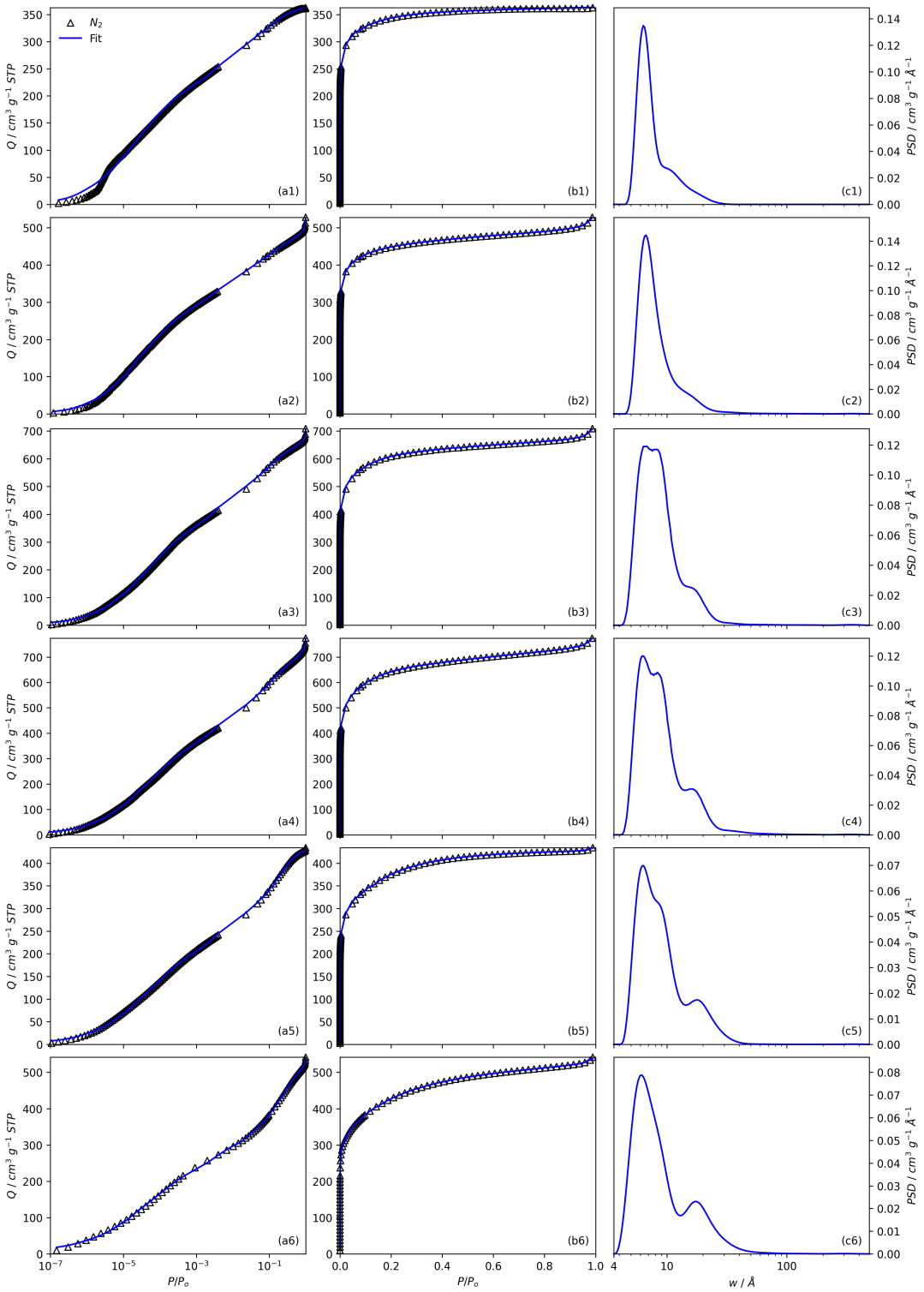

Figure S1.8 Fits to N_2 isotherms with logarithmic (column a) and linear (column b) relative pressure scale, and resultant differential PSDs (column c) for samples PU050-600, PU050-700, PU050-800, PU050-900, PU100-800, PU100-900 in order in rows (1-6).

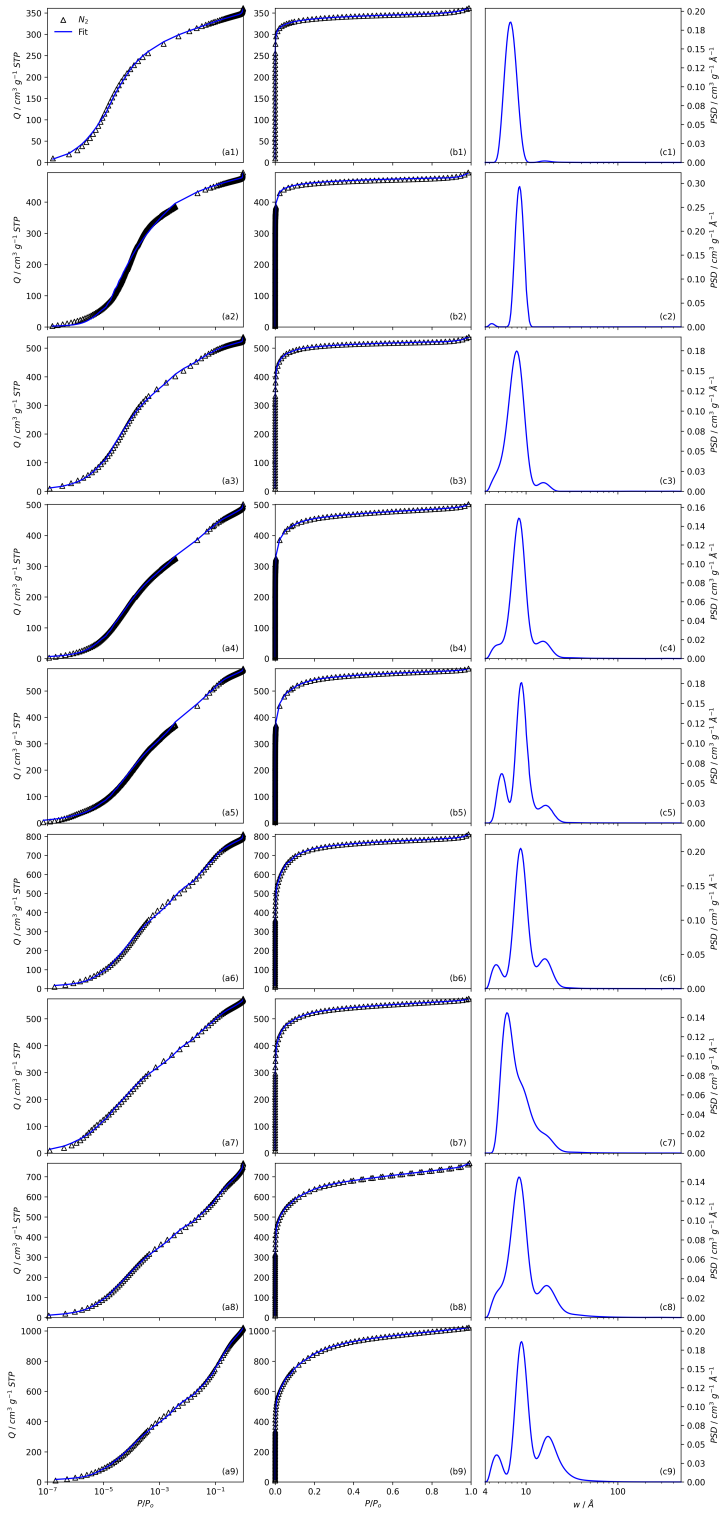

Figure S1.9 Fits to N_2 isotherms with logarithmic (column a) and linear (column b) relative pressure scale, and resultant differential PSDs (column c) for samples aT-2600, aT-2700, aT-2800, aT-2800, aT-4600, aT-4700, aT-4800, aT-6600, aT-6700, aT-6800 in order in rows (1-9).

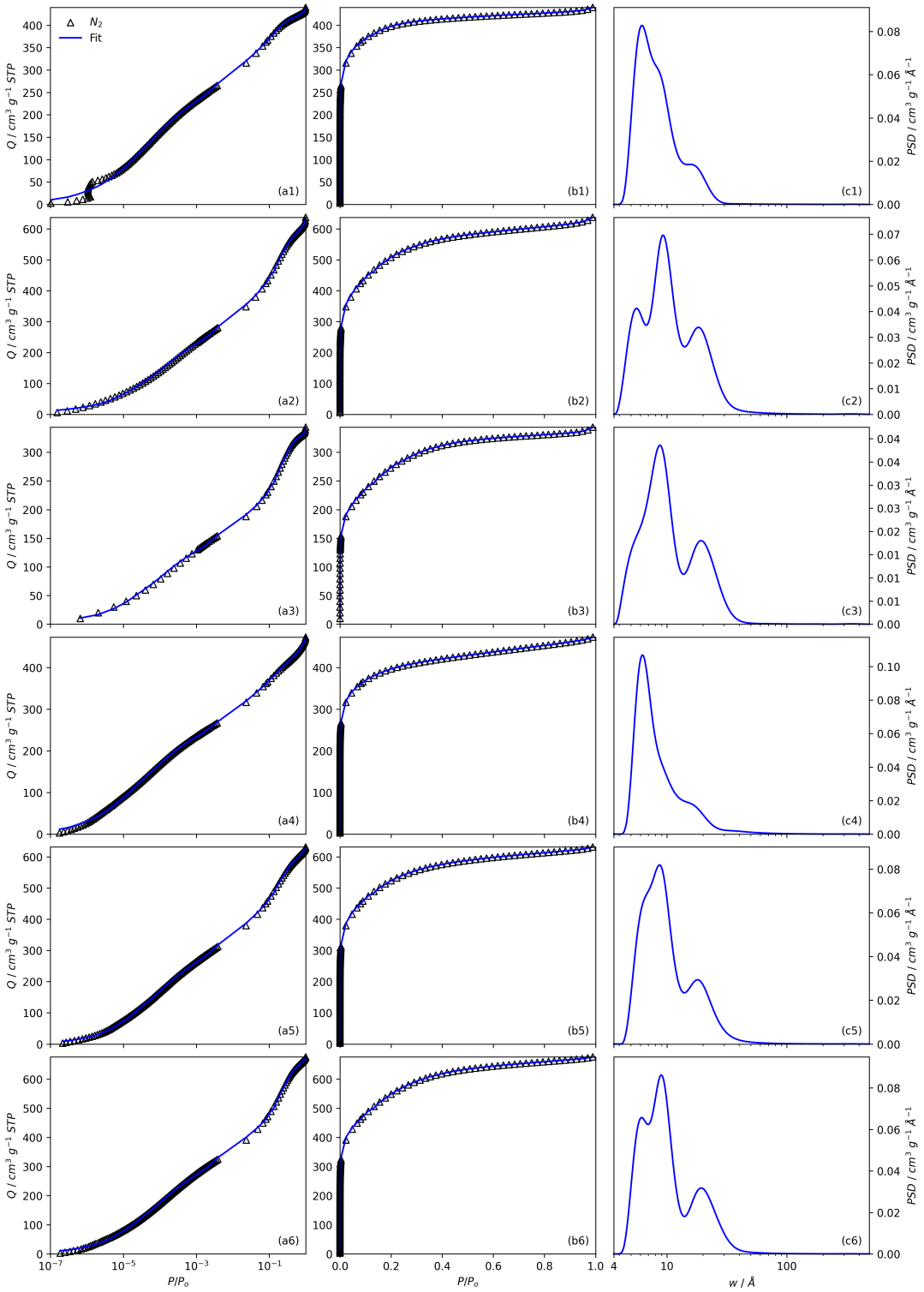

Figure S1.10 Fits to N_2 isotherms with logarithmic (column a) and linear (column b) relative pressure scale, and resultant differential PSDs (column c) for samples hD-4600, hD-4700, hD-4800, hC-4600, hC-4700, hC-4800 in order in rows (1-6).

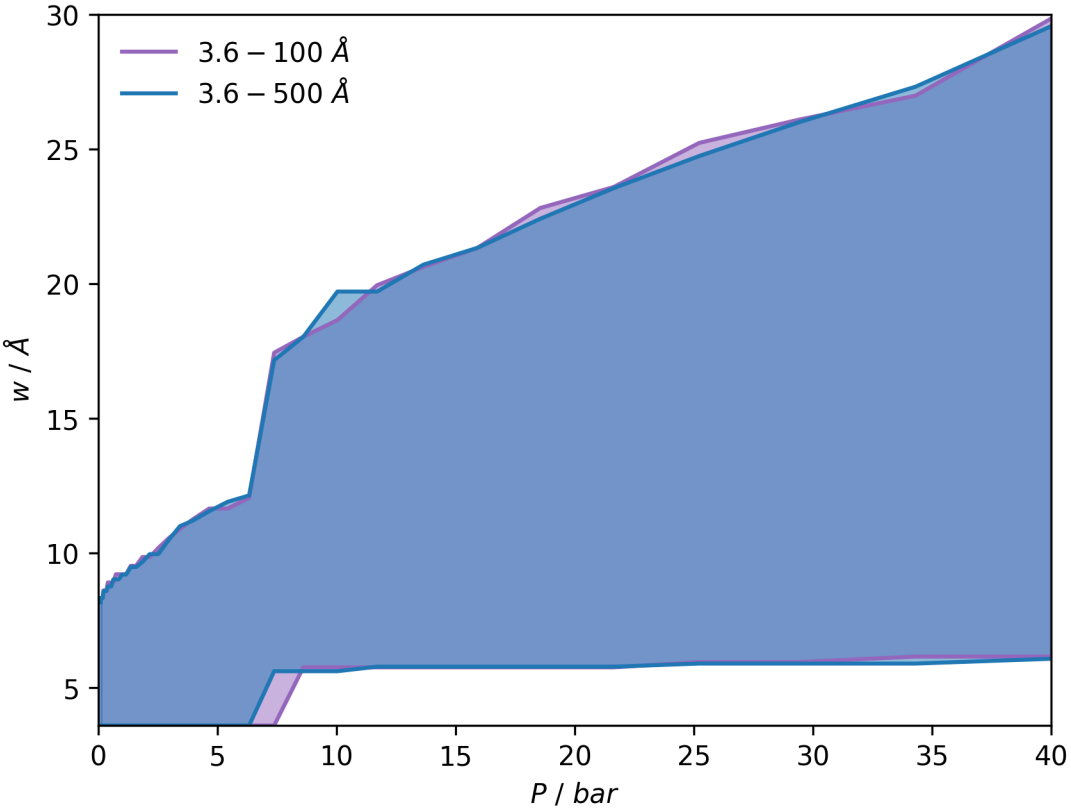

Figure S1.11 Comparison of Ω_V when D_π is calculated from 3.6-100 and 3.6-500 Å using 100 and 500 widths, respectively.

S2 Dataset 2

Sample code: *PPy.y-(HHH)*
Where *PP* denotes precursor(s); see table below. *y.y* s the ratio of porogen (KOH or $NaOOCCH_2$) to precursor. *HHH* is only used for SD samples, and signifies the hydrothermal carbonisation temperature. More detailed information found in original paper. [1]

Table S2.1 Synthetic information and PSD fitting parameter, λ for samples in dataset 2

Prefix	Number of samples	Precursor	Notes	λ
NC	4	Sodium carboxymethyl cellulose	*y.y* determined by degree of substitution	3.5
SD	8	Eucalyptus sawdust	Prepared by hydrothermal carbonisation with KOH at weight ratio defined by *y.y* prior to activation	4.0

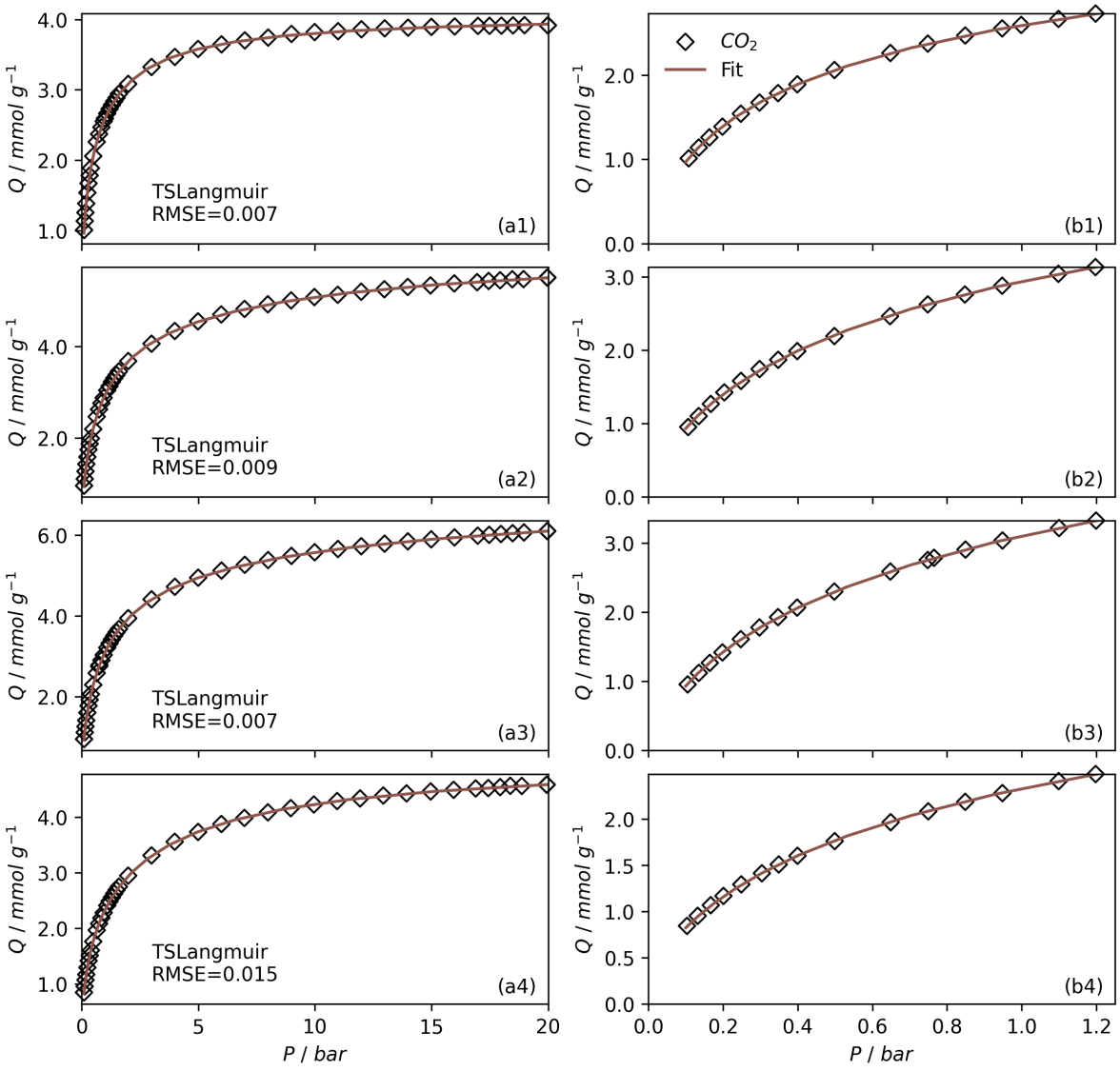

Figure S2.1 CO_2 uptake isotherms and fits in the range 0-20 and 0-1 bar, column (a) and (b) respectively for samples NC0.0, NC0.7, NC0.9, and NC1.2 in order in rows (1-4).

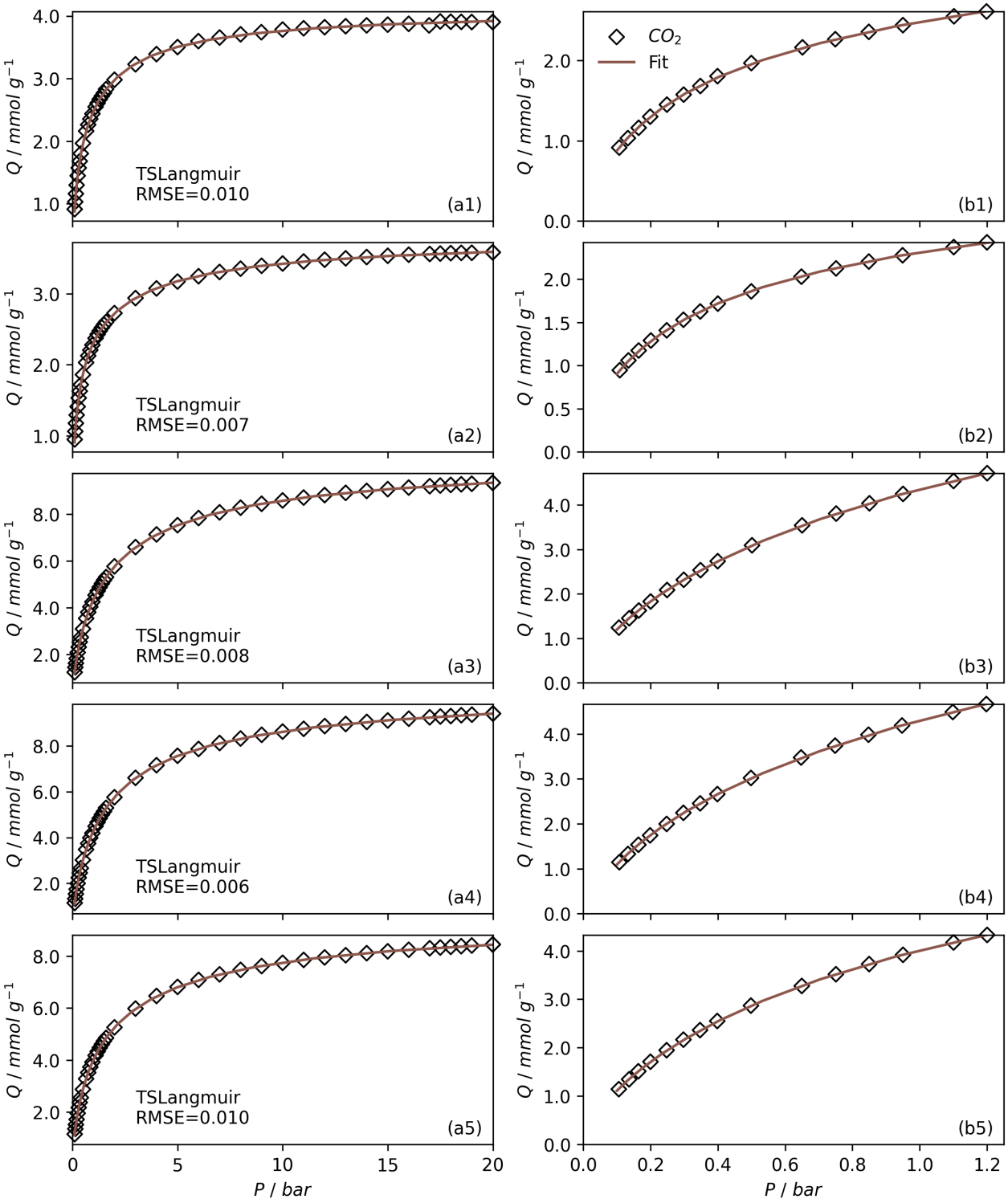

Figure S2.2 CO_2 uptake isotherms and fits in the range 0-20 and 0-1 bar, column (a) and (b) respectively for samples SA0.0-250, SA0.0-300, SA0.5-200, SA0.5-250, SA0.5-300 in order in rows (1-5).

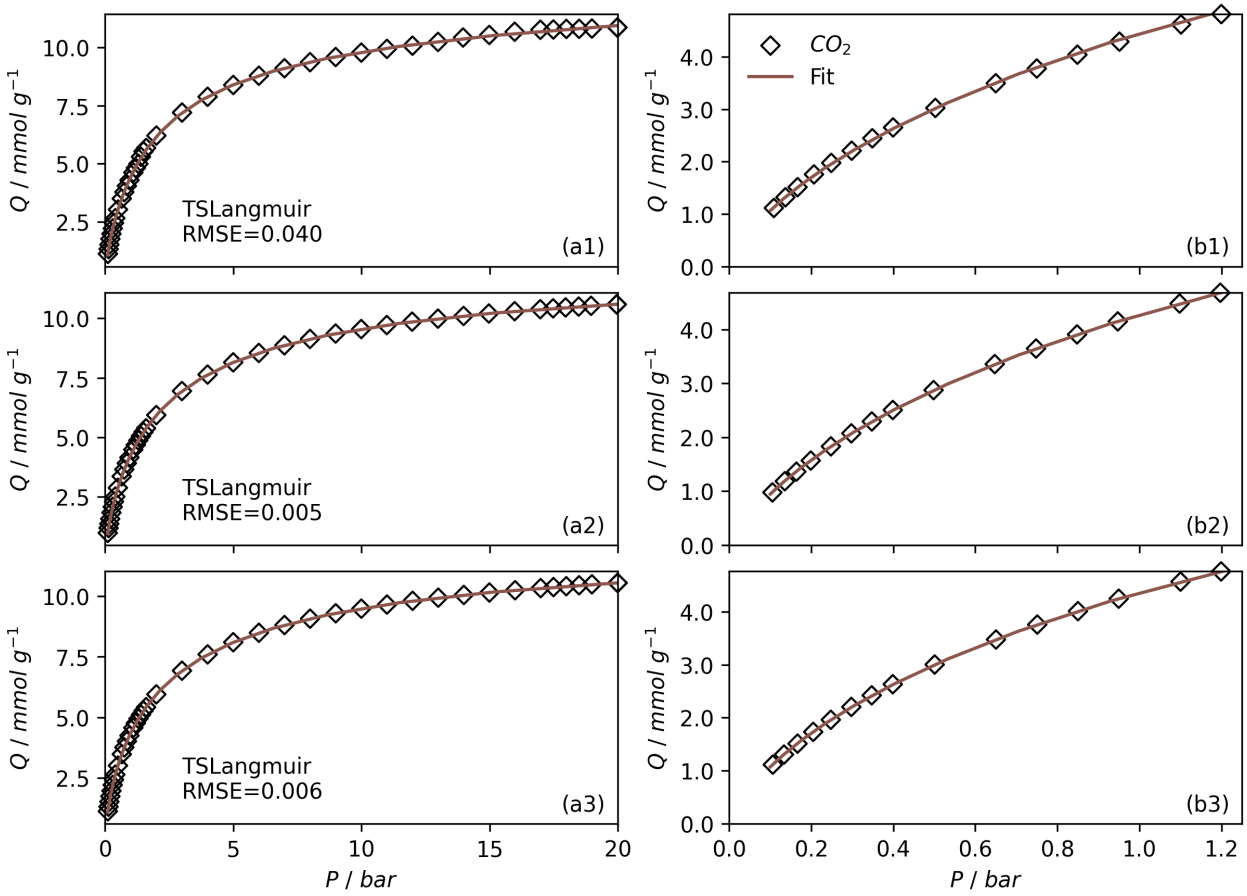

Figure S2.3 CO_2 uptake isotherms and fits in the range 0-20 and 0-1 bar, column (a) and (b) respectively for samples SA1.0-200, SA1.0-250, SA1.0-300 in order in rows (1-3).

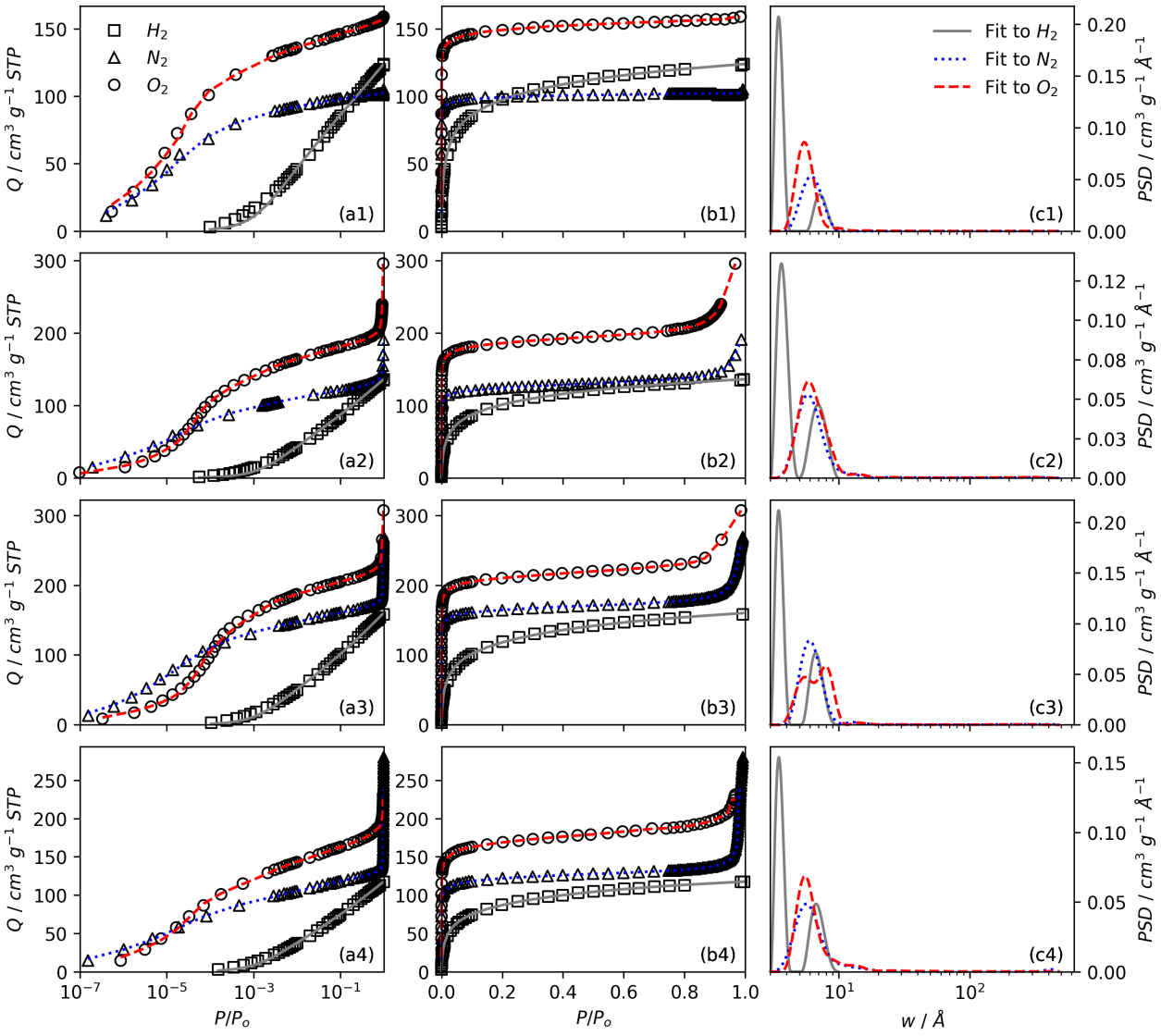

Figure S2.4 Individual fits to H_2, N_2, and O_2 isotherms with logarithmic (column a) and linear (column b) relative pressure scale, and resultant differential PSDs (column c) for samples NC0.0, NC0.7, NC0.9, and NC1.2 in order in rows (1-4).

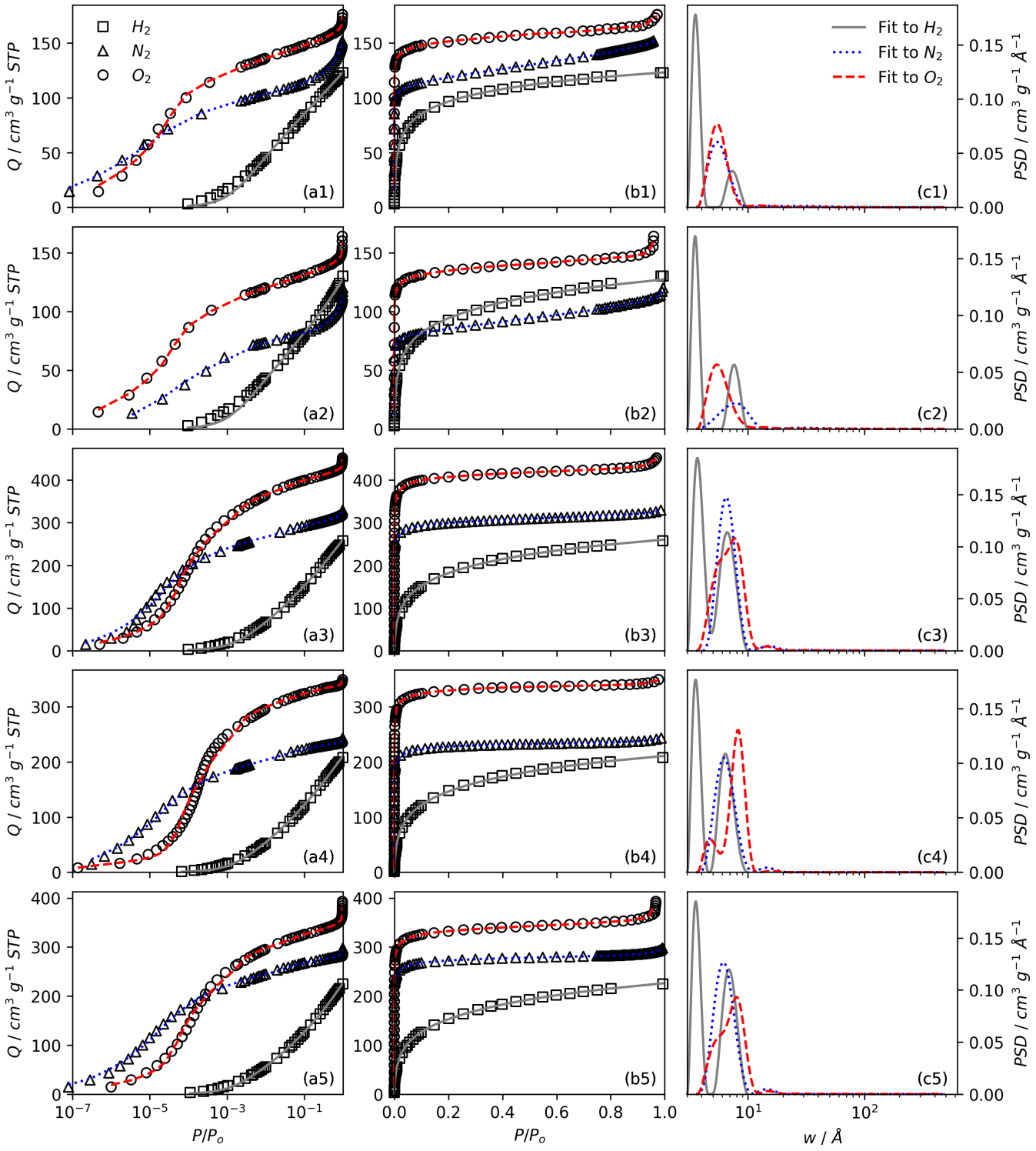

Figure S2.5 Individual fits to H_2, N_2, and O_2 isotherms with logarithmic (column a) and linear (column b) relative pressure scale, and resultant differential PSDs (column c) for samples SA0.0-250, SA0.0-300, SA0.5-200, SA0.5-250, SA0.5-300 in order in rows (1-5).

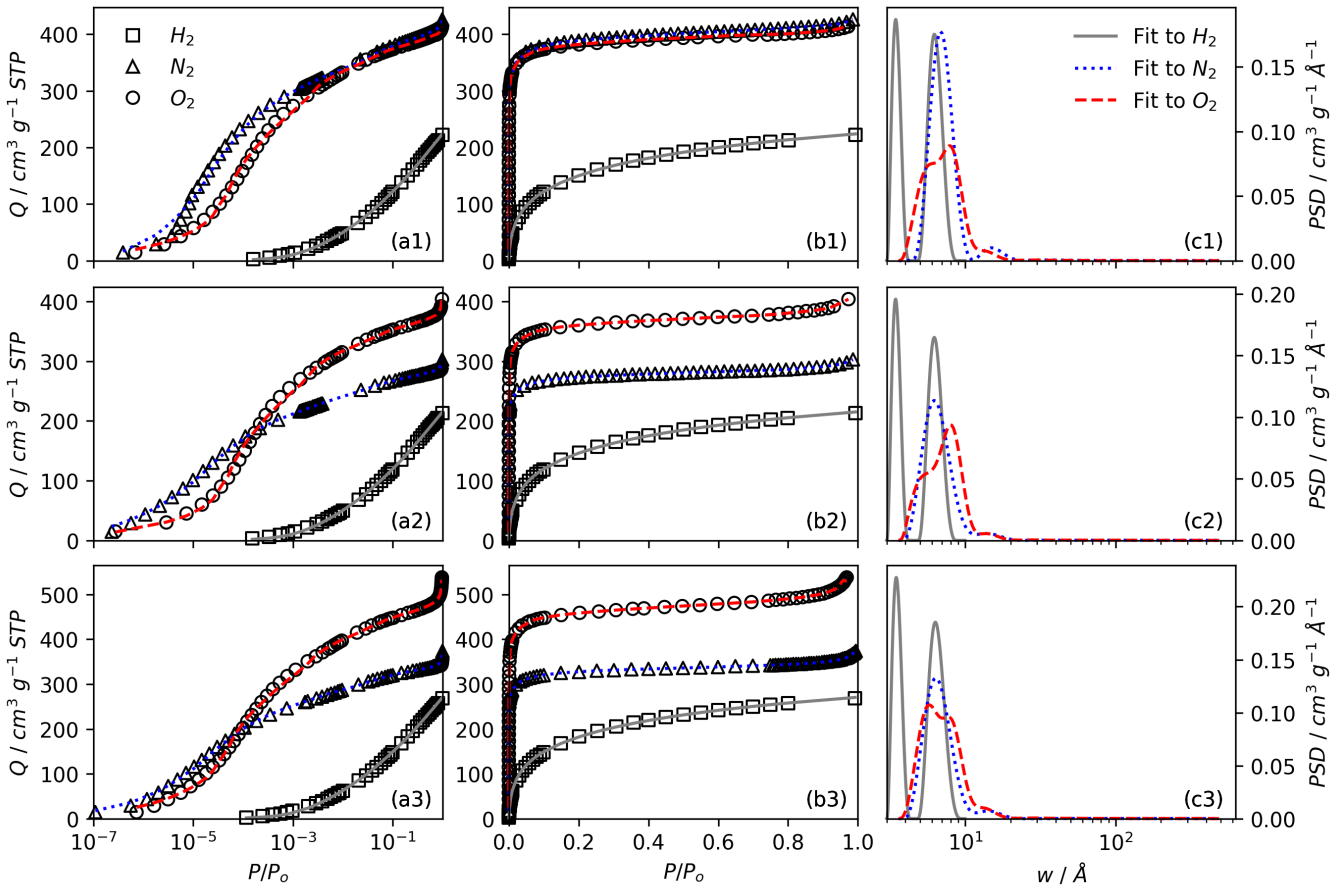

Figure S2.6 Individual fits to H_2, N_2, and O_2 isotherms with logarithmic (column a) and linear (column b) relative pressure scale, and resultant differential PSDs (column c) for samples SA1.0-200, SA1.0-250, SA1.0-300 in order in rows (1-3).

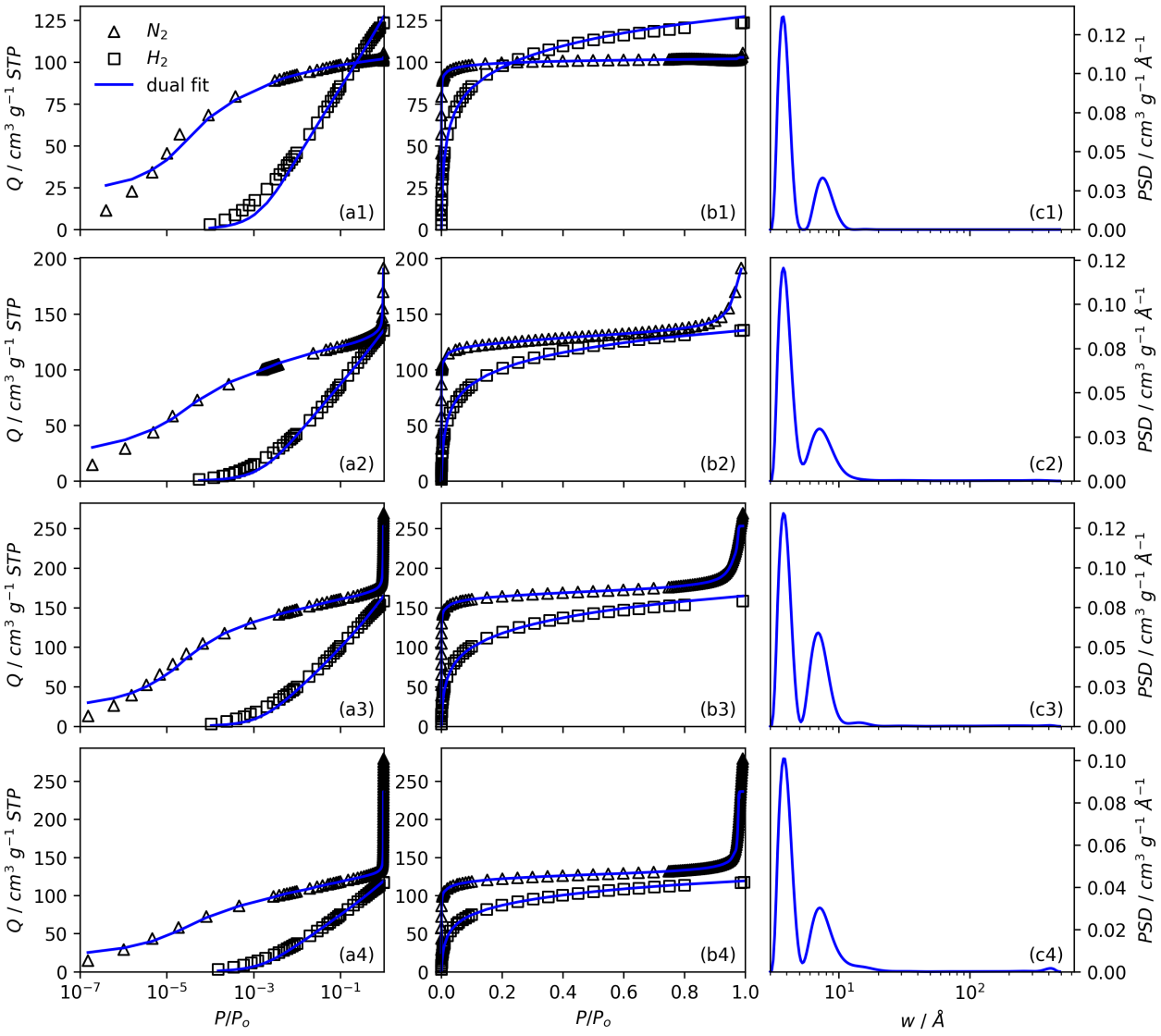

Figure S2.7 Dual fits to N_2, and H_2 isotherms with logarithmic (column a) and linear (column b) relative pressure scale, and resultant differential PSDs (column c) for samples NC0.0, NC0.7, NC0.9, and NC1.2 in order in rows (1-4).

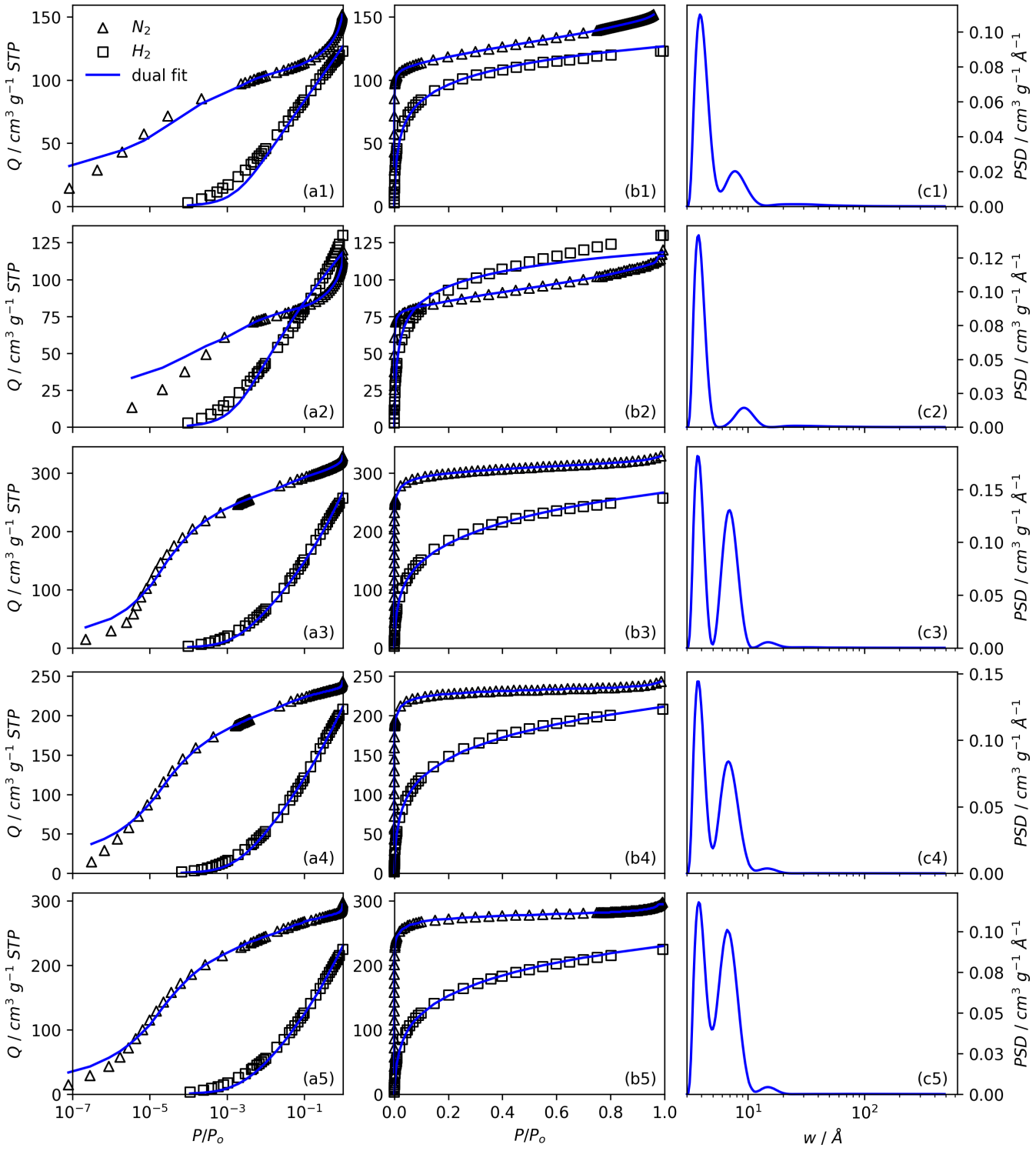

Figure S2.8 Dual fits to N_2, and H_2 isotherms isotherms with logarithmic (column a) and linear (column b) relative pressure scale, and resultant differential PSDs (column c) for samples SA0.0-250, SA0.0-300, SA0.5-200, SA0.5-250, SA0.5-300 in order in rows (1-5).

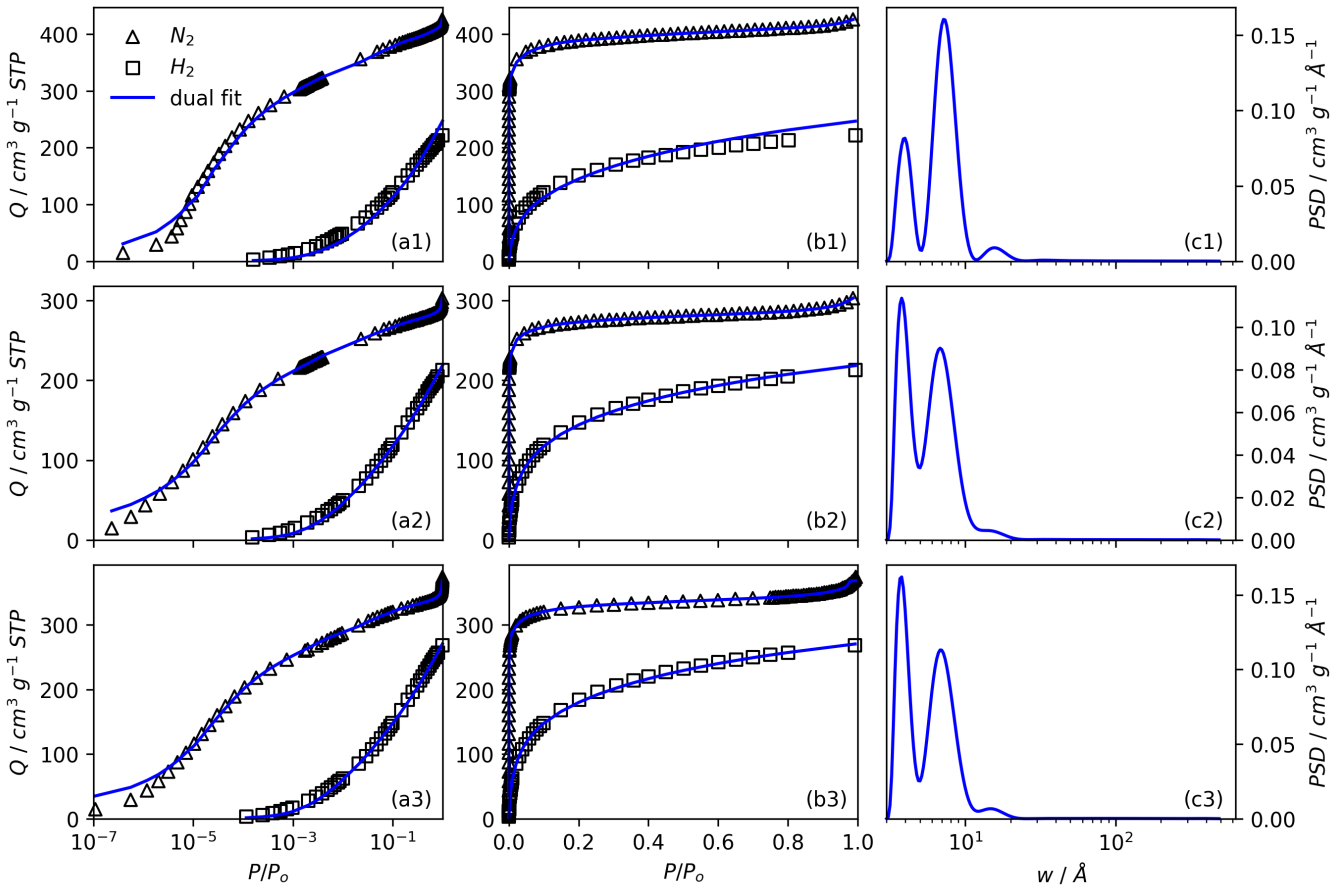

Figure S2.9 Dual fits to N_2, and H_2 isotherms with logarithmic (column a) and linear (column b) relative pressure scale, and resultant differential PSDs (column c) for samples SA1.0-200, SA1.0-250, SA1.0-300 in order in rows (1-3).

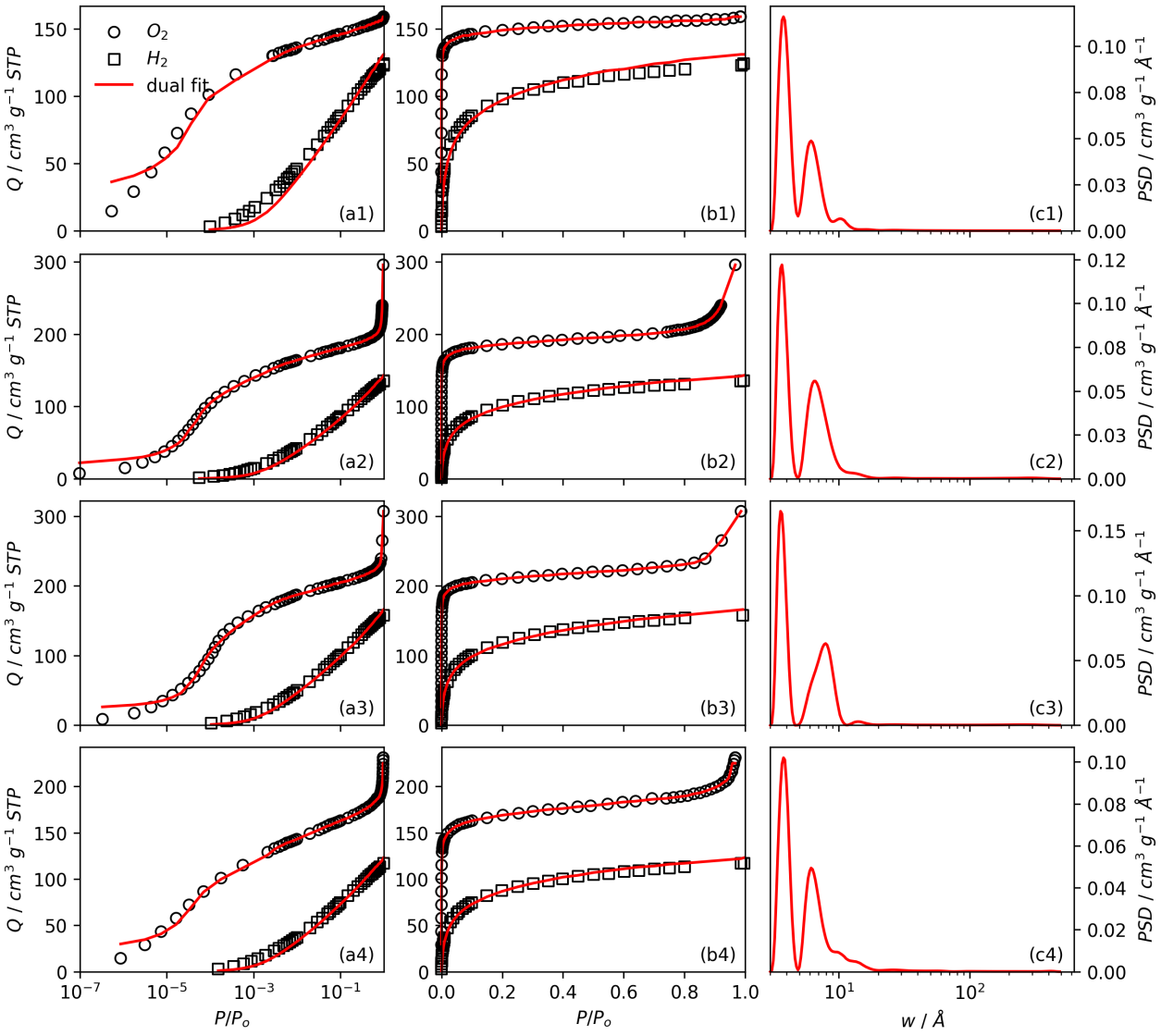

Figure S2.10 Dual fits to O_2, and H_2 isotherms with logarithmic (column a) and linear (column b) relative pressure scale, and resultant differential PSDs (column c) for samples NC0.0, NC0.7, NC0.9, and NC1.2 in order in rows (1-4).

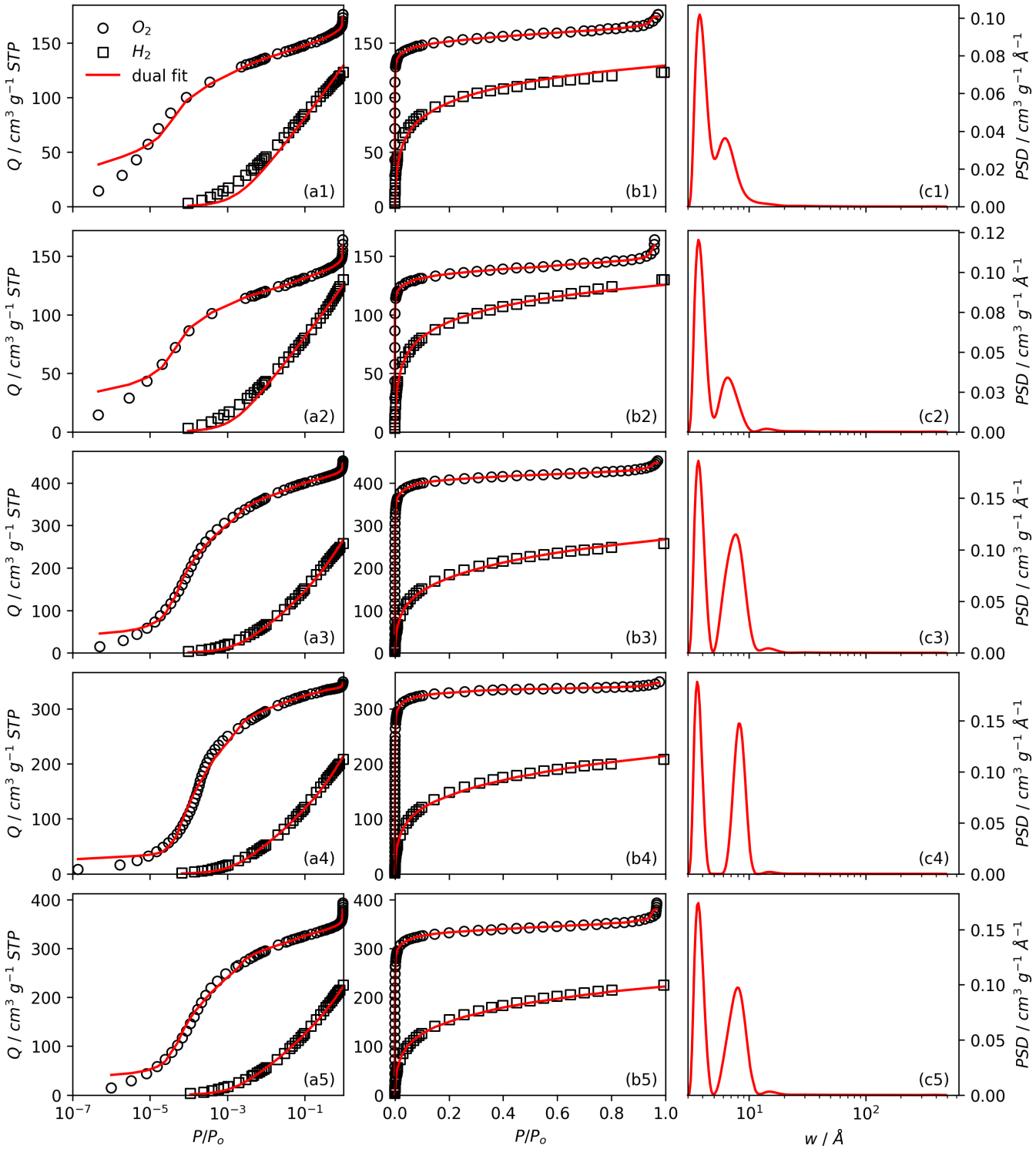

Figure S2.11 Dual fits to O_2, and H_2 isotherms isotherms with logarithmic (column a) and linear (column b) relative pressure scale, and resultant differential PSDs (column c) for samples SA0.0-250, SA0.0-300, SA0.5-200, SA0.5-250, SA0.5-300 in order in rows (1-5).

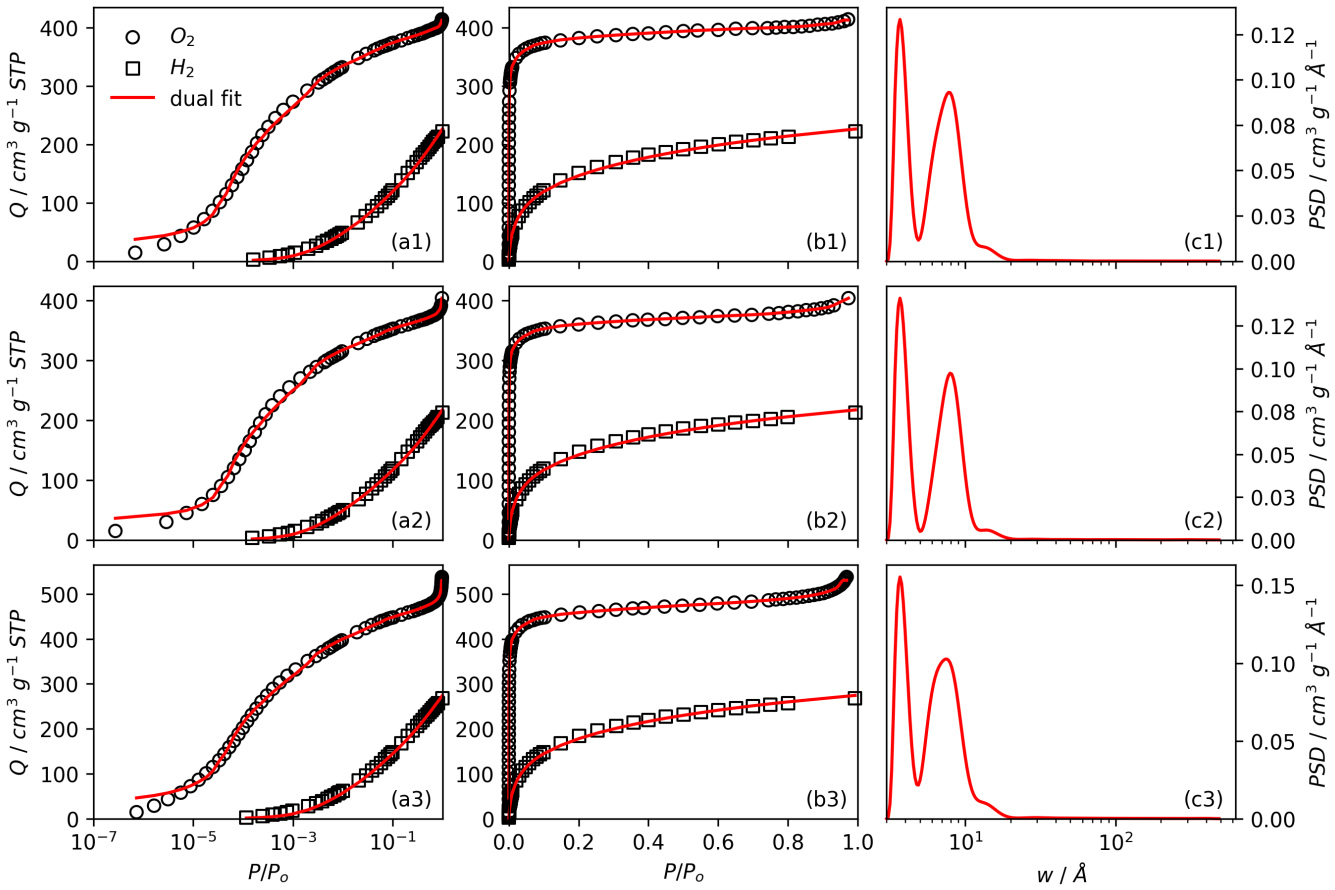

Figure S2.12 Dual fits to O_2, and H_2 isotherms with logarithmic (column a) and linear (column b) relative pressure scale, and resultant differential PSDs (column c) for samples SA1.0-200, SA1.0-250, SA1.0-300 in order in rows (1-3).

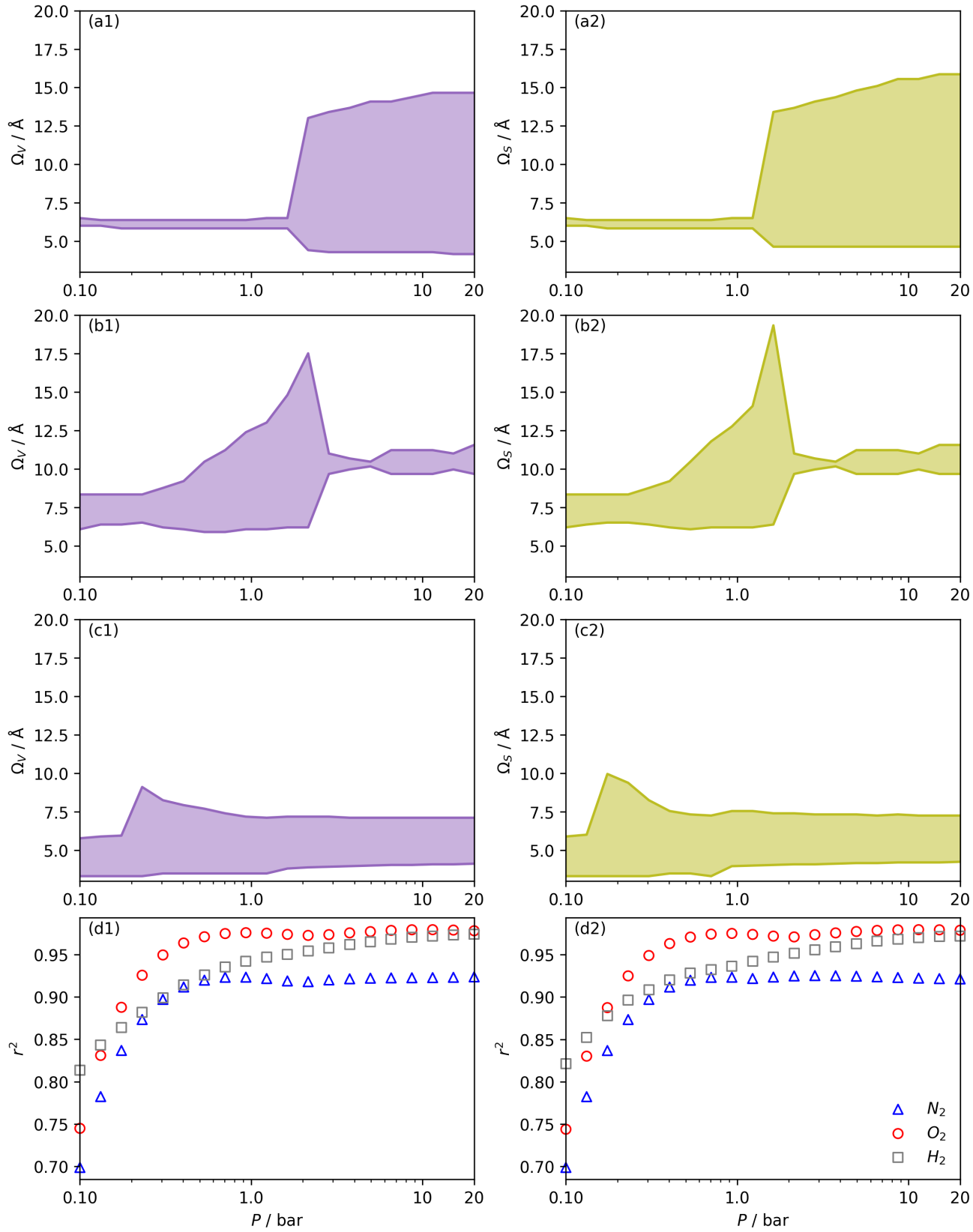

Figure S2.13 : Ω_V (column 1) and Ω_S (column 2) calculated using PSDs N_2 (row a), O_2 (row b), and H_2 (row c) isotherms as well as corresponding r^2 values (row d).

Notes and references

[1] L. S. Blankenship, J. Jagiello and R. Mokaya, *Materials Advances*, 2022, **3**, 3961–3971.